

# Verification of a Motion Cueing Strategy for Stall Recovery Training in a Commercial Transport Simulator

Peter M. T. Zaal\*

*San Jose State University  
NASA Ames Research Center  
Moffett Field, CA 94035*

William W. Chung<sup>†</sup>

*American Systems  
NASA Ames Research Center  
Moffett Field, CA 94035*

Diane M. Carpenter<sup>‡</sup>

*Flight Research Associates  
NASA Ames Research Center  
Moffett Field, CA 94035*

Kevin Cunningham<sup>§</sup> and Gautam H. Shah<sup>¶</sup>

*NASA Langley Research Center  
Hampton, VA 23681*

This paper verifies a motion cueing strategy for improved pilot stall recovery training in commercial transport simulators. Eight airline transport pilots flew a high-altitude stall recovery task in the NASA B747 level-D-certified full flight simulator under three different motion configurations: no motion, baseline motion, and enhanced motion. For each motion condition, pilots performed the task with both baseline aircraft dynamics and aircraft dynamics enhanced with lateral-directional characteristics of the airplane at angle of attack approaching stall. Motion configuration significantly affected: 1) pilot opinions on the helpfulness of motion in performing the task, 2) the maximum roll angle in the stall maneuver, 3) the minimum load factor in the recovery, 4) the number of secondary stick shakers in the stall recovery, and 5) the maximum airspeed in the recovery. The two different aircraft dynamics significantly affected: 1) pilot opinions on the noticeability of the banking roll off near the stall and 2) the maximum roll angle in the stall maneuver. These results indicate that the relatively minor enhancements to the motion logic of heritage commercial transport simulators presented here can significantly improve pilot performance in simulated stall recoveries, and potentially improve stall recovery training.

## I. Nomenclature

|          |   |   |
|----------|---|---|
| $A_s$    | = | stick shaker activation                                   |
| $a_{cg}$ | = | center of gravity linear accelerations, ft/s <sup>2</sup> |
| $a_{ps}$ | = | pilot station linear accelerations, ft/s <sup>2</sup>     |
| $Cl_p$   | = | roll damping linear derivative, rad <sup>-1</sup>         |
| $df$     | = | statistical test degree of freedom                        |
| $F$      | = | analysis-of-variance test statistic, –                    |

---

\*Senior Research Engineer, Human Systems Integration Division, Mail Stop 262-2, peter.m.t.zaal@nasa.gov, Senior Member.

<sup>†</sup>Simulation Engineer, SimLabs, Mail Stop 243-6, william.w.chung@nasa.gov.

<sup>‡</sup>Simulation Engineer, SimLabs, Mail Stop 243-6, diane.m.carpenter@nasa.gov.

<sup>§</sup>Senior Research Engineer, Flight Dynamics Branch, Mail Stop 308, kevin.cunningham@nasa.gov, Senior Member.

<sup>¶</sup>Senior Research Engineer, Flight Dynamics Branch, Mail Stop 308, gautam.h.shah@nasa.gov, Associate Fellow.

|                    |   |  |
|--------------------|---|--|
| $h$                | = | altitude, ft   |
| $K_{\delta a}$     | = | aileron effectiveness gain, –                                    |
| $K_t$              | = | center of gravity translational acceleration gain, –             |
| $K_r$              | = | linear accelerations due to rotations gain, –                    |
| $N_s$              | = | number of secondary stick shakers                                |
| $mr$               | = | motion rating, %   |
| $n$                | = | load factor, –   |
| $p$                | = | probability of observing an effect                               |
| $q1, q2, q3$       | = | questionnaire responses  |
| $r_{cg-ps}$        | = | distance between the center of gravity and the pilot station, ft |
| $V_{CAS}$          | = | calibrated airspeed, kts   |
| $x$                | = | longitudinal distance, NM  |
| $\alpha$           | = | angle of attack, deg   |
| $\Delta C l_{asy}$ | = | rolling moment increment due to aerodynamic stall asymmetry, –   |
| $\Delta h$         | = | altitude loss, ft  |
| $\delta T$         | = | throttle angle, deg  |
| $\theta$           | = | aircraft pitch angle, deg  |
| $\phi$             | = | aircraft roll angle, deg   |
| $\chi^2$           | = | Friedman test statistic, –                                       |
| $\omega$           | = | aircraft rotational rates, rad/s                                 |

## II. Introduction

THIS paper presents an experiment conducted in a level-D-certified B747-400 full flight simulator at NASA Ames Research Center to verify a motion cueing strategy for stall recovery training. Today, airline pilots only receive training in recognizing and recovering from an approach to stall, but not in full stall recovery. Starting in 2019, airline pilots will be required to perform full stall recovery training in flight simulators [1]. Historically, training simulators weren't required to provide training at conditions outside their normal flight envelope, such as at angles of attack above the stall warning threshold. Post-stall aircraft models are generally required to be implemented to simulate the aircraft response after the stall point [2–6]. In addition, motion cues need to adequately represent this response to ensure the skills learned in simulator training are directly usable in real flight.

Under NASA's Airspace Operations and Safety Program, the Technologies for Airplane State Awareness (TASA) subproject conducts research to support the Commercial Aviation Safety Team (CAST) Safety Enhancement 209 (SE209) to study simulator fidelity improvements for commercial aircraft stall training [7]. Under this SE209 research, four simulator studies with pilots were conducted in the Vertical Motion Simulator (VMS) at NASA Ames Research Center, to develop a hexapod motion cueing strategy for stall recovery training in commercial transport simulators [8–11]. This motion cueing strategy prioritizes translational accelerations as a result from rotating around the aircraft's center of gravity over translational accelerations of the center of gravity, allowing for a higher fidelity of the motion cues that directly help a pilot damp the flight path response in a stall recovery, as well as stabilize the progressively less-stable roll dynamics and roll off near stall.

While novel motion algorithms have been proposed in the past, showing promising motion fidelity improvements for upset recovery training, they would require drastic modifications to existing commercial transport simulator motion algorithms and elaborate motion tuning [12, 13]. The motion cueing strategy discussed here only requires minor modifications to existing motion algorithms. The previous VMS experiments simulated a typical hexapod simulator and showed that pilots control more similarly to how they would under full aircraft motion using the new motion cueing strategy; however, these experiments used general aviation pilots in more structured tasks [10, 11]. This paper verifies the usefulness of the proposed motion cueing strategy with eight airline pilots in a level-D-certified full flight simulator using a high-altitude stall recovery task. To increase the operational relevance of this work, modifications were made to the aircraft dynamic model to represent a generic 4-engine transport airplane at stall/post-stall angle of attack.

This study contained several unique elements which differentiate the findings from previous research, and therefore contributes knowledge to the current literature. First, it is the first study to test a new motion cueing strategy for stall recovery training in a level-D-certified full flight simulator. Second, it does so in conjunction with rudimentary generic modifications to a type specific aircraft model typically used in most heritage simulators. Third, it used a very large, generally stable, four-engine transport aircraft with eight commercial airline pilots.

The paper is structured as follows. The high-altitude stall recovery task used in this study is described in Section III, after which the simulator’s aircraft dynamic model and motion logic modifications are discussed in Section IV. Section V discusses the experimental setup. The results are provided in Section VI, followed by a discussion and conclusions in Sections VII and VIII, respectively.

### III. High-Altitude Stall Recovery Task

The goal of this study was to investigate if relatively minor modifications to the motion logic of a level-D full flight simulator provide improved pilot performance in simulated stall recovery tasks. In addition, the effects of aircraft model enhancements which better represent lateral-directional aircraft behavior at high angles of attack, and the interactions with simulator motion, were investigated. To that extent, a high-altitude stall recovery task was designed that evaluated if changes in motion cues affect pilots’ recovery performance by helping a pilot damp the flight path response, as well as stabilize the increasingly unstable roll dynamics and roll-off near stall. The task was very similar to a high-altitude stall recovery task previously utilized in the VMS [14]. Fig. 1 provides the flight card for the task as a representative example of the instructions provided to pilots.

The task started during cruise at 210 kts at an altitude of 36,000 ft. To increase pilots’ taskload, moderate turbulence was present throughout the task. In addition, the task was performed in the clouds; that is, without any visual attitude references from the out-the-window view. Pilots were instructed to initiate a self-induced stall by setting the throttles to idle and pitching approximately 15 deg nose up, decelerating through the stick shaker. To make sure pilots initiated the stall recovery under the same full-stall conditions, the autopilot disconnect tone sounded when the critical angle of attack was reached and a sink rate was developed [5]. Pilots were not to recover until the tone sounded.

To recover from the stall, pilots had to follow the correct recovery sequence of reducing the angle-of-attack (by pitching to approximately 15 deg nose down), leveling the wings, and applying full throttle until establishing a safe positive climb rate [15]. The task called for the pilots to pull the nose up gently and smoothly so as not to activate the stick shaker during the recovery. Pilots were allowed to use the pitch trim at their own discretion. So that all pilots reached a consistent end state in the recovery, the task run terminated automatically when they were no longer descending ( $\dot{h} > 0$ ), were at least as fast as their starting speed ( $V_{cas} \geq 210$  kt), and the wings were level ( $|\phi| < 5$  deg).

Example recordings for aircraft altitude, pitch, roll, throttle angle, angle of attack, calibrated airspeed, load factor, and stick shaker activation during one run of the task are provided in Fig. 2. The start of the stall maneuver is depicted by the first dashed line, while the moment the stall indication tone sounded is depicted by the second dashed line. During the approach to stall, the altitude increased, airspeed decreased, and angle of attack increased gradually. Note that in these specific flight conditions, the stick shaker activated around an angle of attack of 12 deg. A right wing roll-off can clearly be observed around when the maximum angle of attack was reached. It can be observed that the pilot followed the correct stall recovery procedure during this run by first lowering the nose, then rolling wings level, and, finally, adding power. No secondary stick shaker activations in the stall recovery were observed during this run.

|   |
|---|
| <p><b>Task:</b> Recover from a high-altitude stall</p> <p><b>Initial Condition:</b> Level at FL360 altitude and 210 kts</p> <p><b>Configuration:</b> clean</p> <p><b>Weight:</b> 450,000 lbs</p> <p><b>Center of gravity:</b> 21.0 % MAC</p> <p><b>Ceiling/visibility:</b> In the clouds</p> <p><b>Wind:</b> None</p> <p><b>Turbulence:</b> Moderate</p> <p><b>Gusts:</b> None</p> <p><b>Procedure:</b></p> <ol style="list-style-type: none"> <li>1) Retard throttles to idle.</li> <li>2) Pull up to approximately 15 deg causing the airspeed to drop.</li> <li>3) Keep the wings level.</li> <li>4) Continue deceleration through stick shaker until a tone sounds indicating the stall.</li> <li>5) Recover by applying approximately 15 deg nose down pitch, roll as needed, power as needed to return to steady-state flight.</li> <li>6) Task evaluation ends when the airspeed is above 210 kts, the aircraft is climbing, and the wings are level.</li> </ol> <p><b>Desired performance:</b></p> <ol style="list-style-type: none"> <li>1) Maintain wings level during entry.</li> <li>2) Proper stall recovery procedure (push, roll, thrust, stabilized flight, in that order).</li> <li>3) Recover to speed <math>&gt; 210</math> kts and positive rate of climb.</li> <li>4) Recover without exceeding aircraft’s limitations.</li> <li>5) Recover with smooth and positive control.</li> <li>6) During recovery, no more than one additional stick shaker activation.</li> </ol> |
|---|

**Fig. 1 Experiment flight card.**

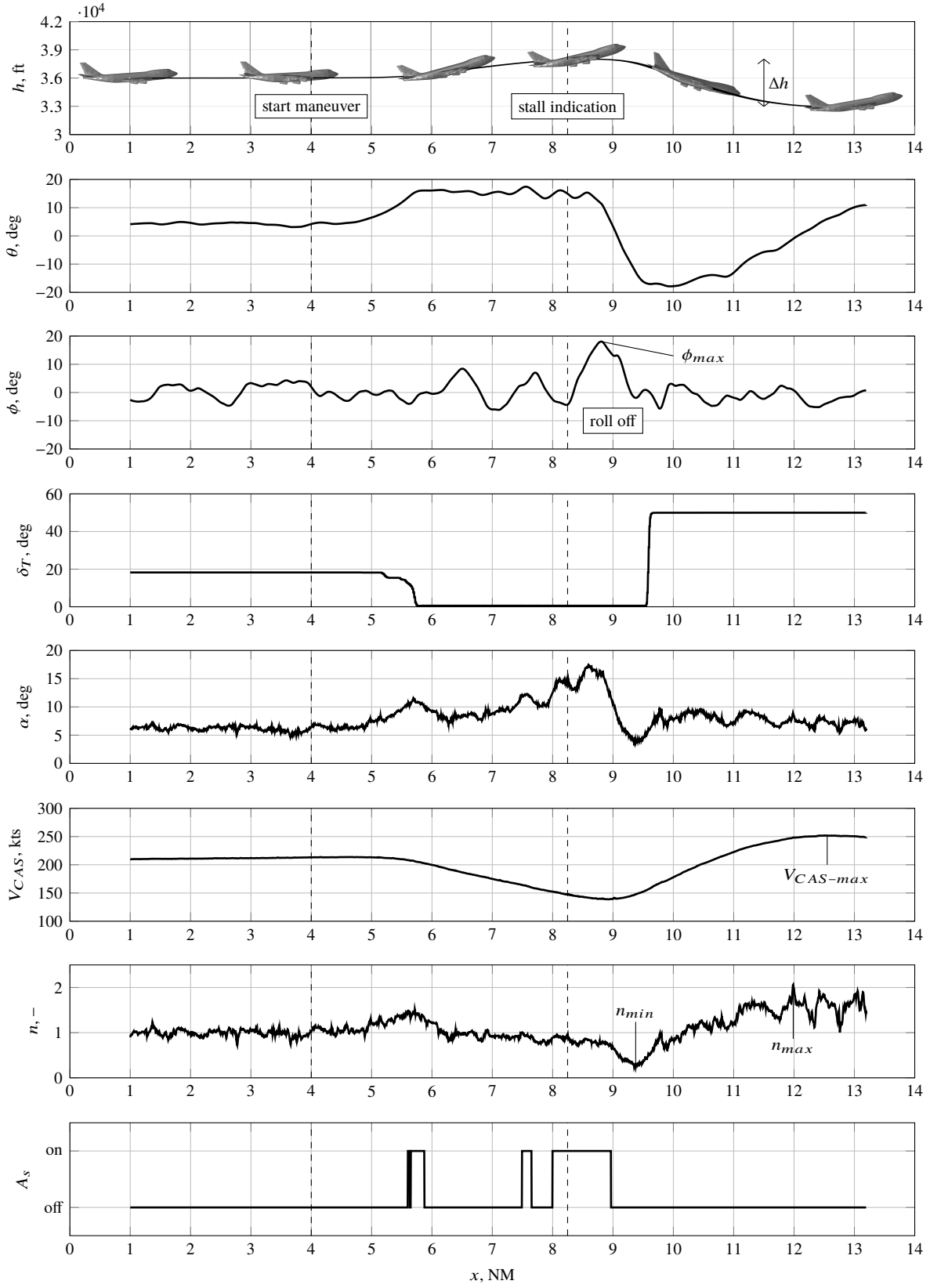


**Fig. 2** Flight variable recordings.

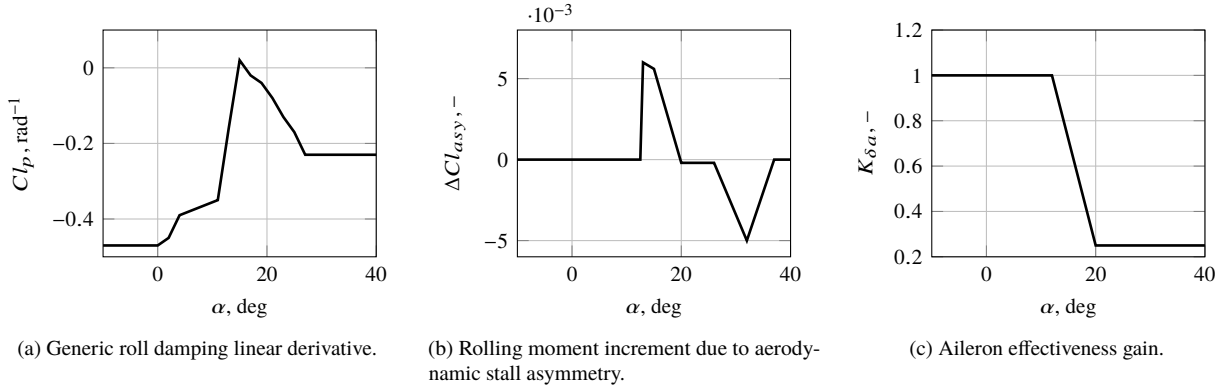


**Fig. 3 Modifications to the aerodynamic model of a very large, generic, four-engine transport airplane.**

## IV. Simulator Modifications

The purpose of the simulator modifications was to enable the investigation of the usefulness of a new simulator motion cueing strategy for stall recovery training developed in previous experiments [11]. For that purpose, modifications to the aircraft dynamic model were implemented to better represent aircraft behavior at high angles of attack. Note that information provided in this section is limited to generic adjustments made by the experimenters due to proprietary elements of the baseline simulator hardware and software.

### A. Aircraft Dynamics

As in most heritage simulators, the existing flight dynamics model was not designed to represent the lateral-directional characteristics of the airplane at angle of attack approaching stall. For the purpose of this study, modifications to the aerodynamic model of a very large, generic, four-engine transport aircraft were developed and incorporated into the existing simulation software (that is, not B747 specific). The aerodynamic modifications were limited to the roll axis (roll damping, aerodynamic asymmetry, and aileron control power). The fidelity of the modifications was intended only to approximate the most dominant stability and control characteristics for the airplane at high angle of attack when in the cruise configuration at sub-sonic flight conditions.

The updates to roll damping, stall asymmetry, and aileron effectiveness are presented in Fig. 3. These data were implemented as linear table lookups. All data shown in Fig. 3 are generic, non-proprietary, and were derived from public sources [16, 17]. The roll damping stability coefficient data in Fig. 3a replaced the roll damping data in the baseline simulation. Effects of Mach number and altitude were not included in this model and were considered to be secondary to the model uncertainty at post-stick-shaker angle of attack. In addition, the effect of slats/flaps on roll damping was not modeled, as the model was intended to be used in a clean wing configuration only. The rolling moment increment due to stall asymmetry was computed from linearly interpolated lookup of the data in Fig. 3b. Adding an asymmetry in roll to the unmodified model required additional pilot workload to control another axis, which is typical of stalls in actual flight, adding realism at a relatively minor cost [5]. These body-axis rolling-moment increments were added to the buildup of the total rolling moment coefficient. The aileron effectiveness gain was linearly interpolated from the data in Fig. 3c. The gain, which varied from 1.00 to 0.25 was used as a multiplier on the rolling moment increment due to aileron deflection.

### B. Motion Cueing

The simulator uses an adaptive motion filter logic to generate motion commands from linear and angular accelerations from the flight equations [18]. A new motion cueing strategy was developed in previous experiments using the VMS [9]. This motion strategy prioritizes translational accelerations as a result of rotations with respect to the center of gravity over translational accelerations of the center of gravity [19]. Minor modifications to the original simulator motion algorithms were required to allow for this motion strategy to be implemented. The main modification was the implementation of gains  $K_l$  and  $K_r$  in the equation for the linear accelerations at the pilot station:

**Table 1 Enhanced motion parameters.**

|                             | Degree of Freedom |      |       |      |       |     |
|-----------------------------|-------------------|------|-------|------|-------|-----|
|                             | Surge             | Sway | Heave | Roll | Pitch | Yaw |
| High-Pass Gains             | 0.7               | 0.7  | 0.7   | 1.0  | 1.0   | 1.0 |
| High-Pass Break Frequencies | 0.6               | 0.6  | 0.6   | 0.3  | 0.3   | 0.3 |
| Low-Pass Gains              | 1.0               | 1.0  | –     | –    | –     | –   |
| Low-Pass Break Frequencies  | 0.6               | 0.6  | –     | –    | –     | –   |

$$a_{ps} = K_t a_{cg} + K_r (\dot{\omega} \times r_{cg-ps} + \omega^2 \times r_{cg-ps}) \quad (1)$$

where  $a_{ps}$  and  $a_{cg}$  are the linear accelerations at the aircraft’s pilot station and center of gravity, respectively, and  $\omega$  are the aircraft rotational rates at the center of gravity. The distance from the center of gravity to the pilot station is  $r_{cg-ps}$ . Finally,  $K_t$  is the newly introduced gain on the c.g. translational accelerations and  $K_r$  is the gain on the linear accelerations due to rotations about the center of gravity. Setting the gain  $K_t$  to zero, eliminating the linear accelerations of the center of gravity, resulted in a motion configuration where far less attenuation of the remaining linear accelerations was required compared to the original motion configuration, leading to significantly increased motion filter gains and reduced break frequencies for all degrees of freedom. Other modifications to the standard motion logic entailed disabling the adaptive nature of the motion algorithms and allowing for online adjustment of the motion filter parameters.

The motion parameters were tuned using test runs with a test pilot. The motion filter parameter values for the enhanced motion configuration for each degree of freedom are provided in Table 1. The damping ratios of all filters were set to 0.707. The gains  $K_t$  and  $K_r$  were set to 0.0 and 1.0, respectively.

## V. Experiment Setup

### A. Independent Variables

The experiment used two independent variables in a full-factorial design: aircraft dynamics (DYN) which had two levels (baseline or enhanced dynamics) and simulator motion (MOT) which contained three levels (no motion, baseline motion, or enhanced motion). The six experimental conditions are presented in Table 2. The baseline aircraft dynamics and motion configuration were the unaltered original dynamics and motion configuration of the simulator. A no-motion condition was included in the experiment as a baseline to ensure that some perspective was kept on potentially small differences between the two motion configurations. In the no-motion condition, the motion of the simulator was washed out completely and no motion effects such as buffeting were present. More details about the enhanced aircraft dynamics and enhanced motion are provided in Section IV.

**Table 2 Experimental conditions.**

| Condition | Aircraft Dynamics | Simulator Motion |
|-----------|-------------------|------------------|
| B1        | baseline          | no motion        |
| B2        | baseline          | baseline         |
| B3        | baseline          | enhanced         |
| E1        | enhanced          | no motion        |
| E2        | enhanced          | baseline         |
| E3        | enhanced          | enhanced         |

### B. Apparatus

The experiment was conducted in the B747-400 Level-D-certified full-flight simulator at NASA Ames Research Center (Fig. 4) [18]. The cab of this simulator includes a flight deck, observer seats, and operator control station. In addition, there is an off-board operator control station from which the simulation was controlled. The simulator was used in its standard hardware configuration. Enhancements to the simulation software were made according to Section IV.



**Fig. 4 B747-400 simulator.**



**Fig. 5 B747-400 cockpit.**

The flight deck is a replication of a B747-400 cockpit (Fig. 5); that is, all instruments, controls, and switches operate in the same way as they do in the actual aircraft. The simulator is equipped with a three-projector collimated out-the-window visual system, hydraulic six-degree-of-freedom motion system, digital control loading system, digital sound and aural cues system, and a fully integrated autoflight system that provides aircraft guidance and control. The cockpit includes a Primary Flight Display (PFD) and Navigation Display (ND) for both the Captain and First Officer, and an Engine Indication and Crew Alerting System (EICAS) display in the middle of the cockpit. The PFD depicted attitude, airspeed, altitude, and vertical speed information, while basic navigation information was displayed on the ND. The EICAS display provided engine data.

The simulator motion system has an actuator stroke length of 54 inches [18]. It can simulate accelerations of  $\pm 1$  g in the vertical direction and  $\pm 0.7$  g in the longitudinal and lateral axes. The maximum excursion is at least  $-37.5$  deg to  $+32.5$  deg in the pitch axis,  $\pm 32$  deg in the roll axis, and  $\pm 37.5$  deg in the yaw axis. The maximum velocities are at least  $\pm 30$  deg/s in the pitch axis and  $\pm 32$  deg/s in the roll and yaw axes. The maximum accelerations are at least  $\pm 250$  deg/s<sup>2</sup> in all three rotational axes.

Pilots used a tablet computer to fill out a questionnaire with four questions after each run. The tablet computer was mounted on the left or right side of the simulator cab, depending on the seat the pilot participant was using, for easy access.

### **C. Procedures**

Pilots were emailed a briefing document and flight card (Fig. 1) before their scheduled session. At the start of the experiment session, pilots received an extensive brief, explaining the task and procedures of the experiment. Pilots were told the experiment contained six experimental conditions with different combinations of aircraft dynamics and simulator motion that represent the actual aircraft behavior with different levels of fidelity. No details were given about the true nature of the conditions. After the briefing, pilots provided their informed consent and filled out a questionnaire. This questionnaire gathered demographic data and information about pilots' understanding of current stall recovery guidelines, stall experience in real aircraft and stall training experience in simulators. The experiment started after a simulator safety briefing.

Pilots flew the experiment from the seat corresponding to their last position flown on the B747. An experimenter was present in the simulator in the opposite seat from the pilot for the first five participants. Pilots performed seven blocks of six runs for a total of 42 runs. In each block except for the first, the six experimental conditions were presented randomly according to a Latin square design. In the first block, the conditions were presented in the order of Table 2 to allow pilots to get used to the enhanced stall dynamics and motion progressively. The first two blocks of six runs were used for training. Data from these two blocks were removed from the analysis. The last five blocks took measurement data to calculate the results. Each block lasted approximately 20 minutes. A short break was taken outside of the simulator cab after three blocks from the start of the experiment. Pilots were told they could take a break at any time. In total the experiment took about three hours to complete, including briefing and breaks.

Pilots started flying the task after a count down from the simulator operator. The task description is provided in

Section III. The run stopped automatically five seconds after the stall recovery criteria were met. After the end of the run, the simulator was reset for the next run, and the pilot answered the post-run questionnaire on the tablet computer (see Section V.E). For some pilots, the simulator motion system stopped functioning occasionally due to excessive accelerations (mostly for condition E3 and occasionally for B3). If this happened, data for that run were discarded and the run was repeated immediately. After completing all simulator runs, the pilot received a debriefing which provided more details about the true nature of the experiment.

#### D. Participants

Eight pilots, seven male and one female, from four different airlines participated. Five pilots were currently a Captain and three a First Officer. The average age was 52.38 years with a standard deviation of 12.14 years. All pilots flew for a part 121 carrier, and were current and qualified as captain or first officer in the B747-400 in the last 60 months. Most pilots were very experienced with ratings on many aircraft types. The average number of flying hours pilots had on a B747 (all variants) was 5081.25 with a standard deviation of 5861.74 hours. The average number of flying hours on other aircraft types was  $7309.38 \pm 6169.03$ . All pilots gave written consent for their participation and received compensation.

All pilots indicated they were aware of the current FAA stall recovery guidelines. All but one had stalled a real aircraft. Four indicated they had stalled a transport aircraft (50%). This number is much higher than generally seen. Several test pilots participated in the experiment which might partially explain this high number; in addition, some pilots may have confused stick shaker activation with stall. Six pilots had aerobatic experience. Finally, seven pilots indicated they had received upset prevention and recovery training in a simulator and six mentioned they had received full-stall recovery training in a simulator.

#### E. Dependent Measures

Four subjective dependent measures and five objective dependent measures were analyzed. The objective measures were calculated from the recorded simulator data which were collected at 30 Hz. Dependent measures were averaged over the five measurement runs per condition for each pilot.

After each run, pilots rated the simulator motion in reference to what they would expect from the PFD,  $mr$ , by moving a digital slider on an analogue fidelity scale. The analogue scale ranged from 0% (no correlation with the PFD) to 100% (good correlation). Next, pilots provided their level of agreement/disagreement with three different statements using a seven-point Likert scale with the following response items: 1) strongly disagree, 2) disagree, 3) somewhat disagree, 4) neutral, 5) somewhat agree, 6) agree, and 7) strongly agree. The first statement,  $q1$ , was “The simulator motion helped me perform this task better.”, the second,  $q2$ , was “There was a noticeable roll off near the stall requiring significant control inputs to counteract.”, and the third,  $q3$ , was “I expect that I would be able to perform a satisfactory high-altitude stall recovery in actual flight if I would train with this aircraft and simulator motion setting.”.

Several objective measures captured the effect of aircraft dynamics and motion on task performance. Many measures related directly to the performance criteria for the high-altitude stall (Fig. 1). Maximum roll attitude,  $\phi_{max}$ , applied to the entire run; that is, approach to stall and stall recovery. Altitude loss,  $\Delta h$ , minimum load factor,  $n_{min}$ , maximum load factor,  $n_{max}$ , number of secondary stick shakers,  $N_s$ , and maximum calibrated airspeed,  $V_{CAS-max}$ , applied to the stall recovery segment. Fig. 2 depicts these objective dependent measures.

### VI. Results

Mean post-run questionnaire and task performance results presented here are from eight pilots. For every pilot, data from the last five runs for each experimental condition were averaged. Error-bar plots present the continuous-interval dependent measures, with means and 95% confidence intervals for each condition. Bar plots present the ordinal dependent measures, with the number of occurrences for each dependent measure level and the median for each experimental condition.

A repeated-measures analysis of variance (ANOVA) detected statistically significant differences in the continuous interval dependent measures [20]. For the ANOVA to produce accurate results, the data must meet three assumptions: 1) there should be no significant outliers, 2) data should be approximately normally distributed for each level of the independent variable, and 3) variances of the differences between all combinations of levels of the independent variable must be equal (that is, assumption of sphericity). Outliers were identified using studentized residuals, normality was checked using the Shapiro-Wilk test, and Mauchly’s test checked the assumption of sphericity. Outliers were considered



**Table 3 Summary of ANOVA test results.**

| Dependent Measures         | Independent Variables |          |          |             |          |          |             |          |          |
|----------------------------|-----------------------|----------|----------|-------------|----------|----------|-------------|----------|----------|
|                            | DYN                   |          |          | MOT         |          |          | DYN×MOT     |          |          |
|                            | <i>df</i>             | <i>F</i> | <i>p</i> | <i>df</i>   | <i>F</i> | <i>p</i> | <i>df</i>   | <i>F</i> | <i>p</i> |
| <i>mr</i>                  | 1.00, 7.00            | 0.003    | 0.961    | 2.00, 14.00 | 3.447    | 0.061    | 2.00, 14.00 | 0.033    | 0.967    |
| $\phi_{max}$               | 1.00, 7.00            | 28.544   | 0.001    | 2.00, 14.00 | 5.009    | 0.023    | 2.00, 14.00 | 1.933    | 0.181    |
| $\Delta h$                 | 1.00, 7.00            | 4.005    | 0.085    | 2.00, 14.00 | 1.824    | 0.198    | 2.00, 14.00 | 0.055    | 0.947    |
| <i>n<sub>min</sub></i>     | 1.00, 7.00            | 0.778    | 0.407    | 2.00, 14.00 | 3.992    | 0.042    | 2.00, 14.00 | 0.386    | 0.687    |
| <i>n<sub>max</sub></i>     | 1.00, 7.00            | 3.141    | 0.120    | 2.00, 14.00 | 0.952    | 0.410    | 2.00, 14.00 | 0.917    | 0.423    |
| <i>V<sub>CAS-max</sub></i> | 1.00, 7.00            | 1.864    | 0.214    | 2.00, 14.00 | 3.809    | 0.048    | 2.00, 14.00 | 0.202    | 0.819    |

■ = significant ( $p < 0.05$ )      □ = not significant ( $p \geq 0.05$ )

**Table 4 Summary of Friedman test results.**

| Dependent Measures   | Independent Variables |          |          |           |          |          |           |          |          |
|----------------------|-----------------------|----------|----------|-----------|----------|----------|-----------|----------|----------|
|                      | DYN                   |          |          | MOT       |          |          | CND       |          |          |
|                      | <i>df</i>             | $\chi^2$ | <i>p</i> | <i>df</i> | $\chi^2$ | <i>p</i> | <i>df</i> | $\chi^2$ | <i>p</i> |
| <i>q1</i>            | 1.00                  | 1.000    | 0.317    | 2.00      | 7.043    | 0.030    | 5.00      | 12.465   | 0.029    |
| <i>q2</i>            | 1.00                  | 34.105   | < 0.001  | 2.00      | 1.118    | 0.572    | 5.00      | 71.267   | < 0.001  |
| <i>q3</i>            | 1.00                  | 0.727    | 0.394    | 2.00      | 4.841    | 0.089    | 5.00      | 9.049    | 0.107    |
| <i>N<sub>s</sub></i> | 1.00                  | 0.310    | 0.577    | 2.00      | 6.867    | 0.032    | 5.00      | 11.291   | 0.046    |

■ = significant ( $p < 0.05$ )      □ = not significant ( $p \geq 0.05$ )

observations where the studentized residual was greater than  $\pm 3$  standard deviations. No outliers were detected in any of the dependent measures. Data were mostly normally distributed. In the very few cases they were not, no corrections were made, as an ANOVA is fairly robust to deviations from normality. The assumption of sphericity was never violated. Post-hoc tests with Bonferroni adjustment were performed for post-hoc comparisons of experimental conditions when the ANOVA test indicated an overall significant difference.

A Friedman test was used for the ordinal-level dependent measures [20]. The non-parametric Friedman test was first conducted with the data collapsed across the aircraft dynamics levels or the motion configuration levels to detect the significant effects introduced by each. This was followed up by a Friedman test with all individual experimental conditions (that is, the uncollapsed data). Post-hoc Wilcoxon tests with Bonferroni correction were performed for pairwise comparisons of experimental conditions when the Friedman test indicated an overall significant difference.

All statistical tests had a significance level of 0.05. Table 3 gives a summary of the ANOVA test results for all the continuous repeated measures (Section V.E). In this table, *df* are the degrees of freedom, *F* is the test statistic, and *p* is the probability of observing an effect. Table 4 provides a summary of the Friedman test results for all the ordinal repeated measures, with *df* the degree of freedom,  $\chi^2$  the test statistic, and *p* the probability of observing an effect.

### A. Subjective Measures

The post-run questionnaire results are depicted in Fig. 6. There was no statistically significant two-way interaction between aircraft dynamics (DYN) and motion configuration (MOT) for the overall motion rating, *mr* (Table 3). In addition, the main effects of aircraft dynamics and motion configuration showed no statistically significant differences in motion rating. However, the main effect of motion configuration approached statistical significance with a higher motion rating for the experimental conditions with motion. Note that pilots generally provided a motion rating higher than zero for the conditions without motion. Furthermore, there might be an indication that the motion was rated lower in the enhanced motion configuration as compared to the baseline motion condition. This insignificant effect is worth mentioning as it was observed in previous experiments [14]. Pilots tend to provide lower motion ratings in conditions with higher fidelity motion when significant atmospheric turbulence is present due to the more abrupt changes in simulator accelerations.

The response to the statement “The simulator motion helped me perform this task better.”, *q1*, was not statistically significantly affected by the aircraft dynamics, but was statistically significantly affected by the motion configuration

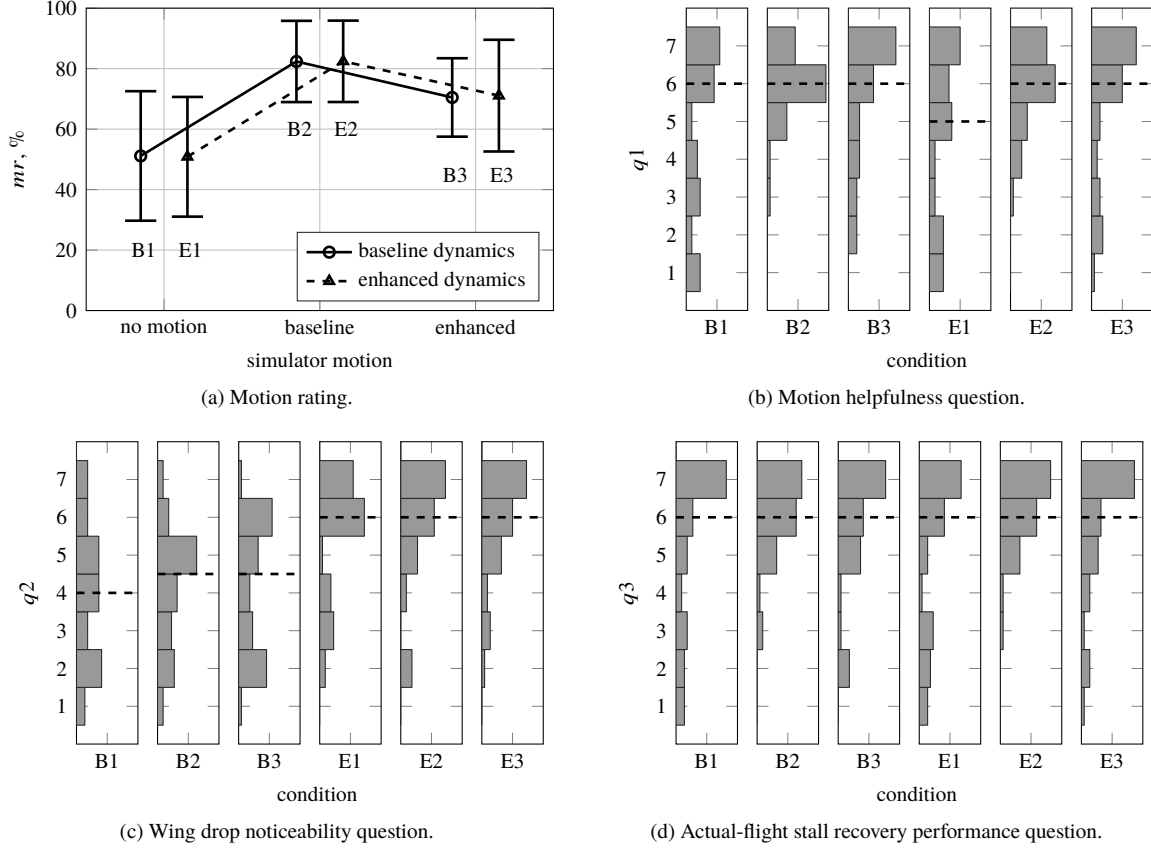


**Fig. 6 Effects of motion setting and aircraft model on subjective measures.**

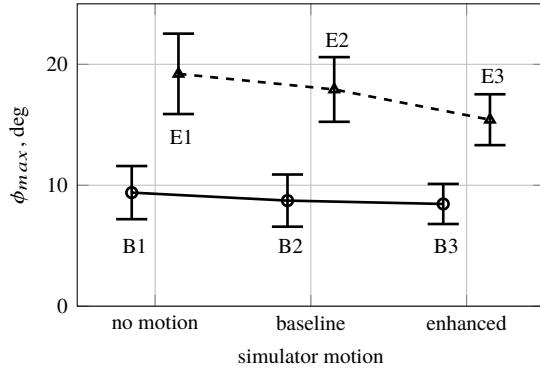
(Table 4). A post-hoc Wilcoxon test with Bonferroni adjustment revealed that the significant difference was between the no-motion and the baseline-motion conditions ( $p = 0.006$ ), with participants agreeing less with this statement without motion compared to baseline motion. The main effect of experimental condition (CND) was also significant (see Table 4). A post-hoc test revealed significant differences between E1 and E2 ( $p = 0.030$ ), and E1 and B2 ( $p = 0.015$ ).

The response to the statement “There was a noticeable roll off near the stall requiring significant control inputs to counteract.”,  $q_2$ , was significantly affected by the aircraft dynamics. Fig. 6c clearly indicates that pilots agreed more strongly with this statement for the conditions with the enhanced aircraft dynamics that included a pronounced banking roll-off (E1-E3) compared to the conditions with the baseline dynamics (B1-B3). The motion configuration did not introduce a statistically significant effect. The main effect of experimental condition was significant and the post-hoc test revealed significant differences between B1 and E1 ( $p < 0.001$ ), B1 and E2 ( $p < 0.001$ ), B1 and E3 ( $p < 0.001$ ), B2 and E1 ( $p < 0.001$ ), B2 and E2 ( $p < 0.001$ ), B2 and E3 ( $p < 0.001$ ), B3 and E1 ( $p < 0.001$ ), B3 and E2 ( $p < 0.001$ ), and B3 and E3 ( $p < 0.001$ ).

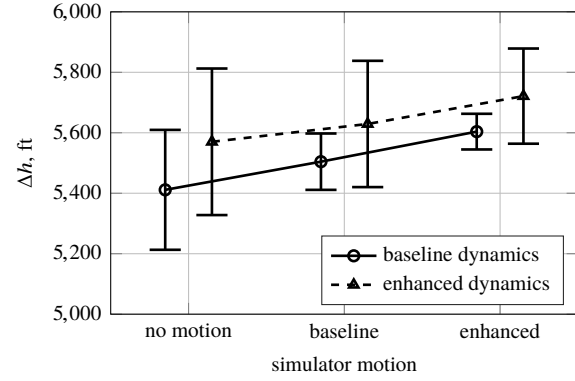
The response to the statement “I expect that I would be able to perform a satisfactory high-altitude stall recovery in actual flight if I would train with this aircraft and simulator motion setting.”,  $q_3$ , was not statistically significantly affected by the independent variables. Pilots agreed strongly with this statement in every experimental condition.

## B. Objective Measures

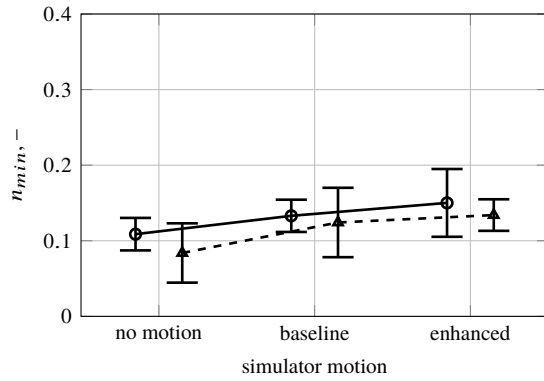
Fig. 7 presents the measures of task performance. No significant interaction between aircraft dynamics and motion configuration was introduced in the maximum roll attitude (Table 3). The maximum roll attitude,  $\phi_{max}$ , was statistically significantly affected by the aircraft dynamics and the motion configuration (Fig. 7a). The maximum roll attitude was significantly higher for the conditions with enhanced aircraft dynamics. In addition, the maximum roll attitude was lower with higher fidelity motion. Post-hoc analysis with Bonferroni adjustment revealed that the maximum roll attitude was significantly lower with enhanced motion compared to no motion ( $p = 0.053$ ).



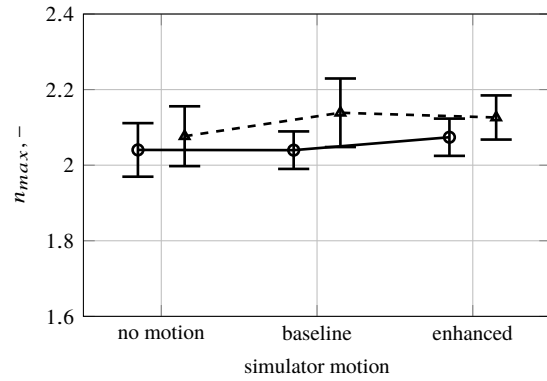
(a) Maximum roll in stall maneuver.



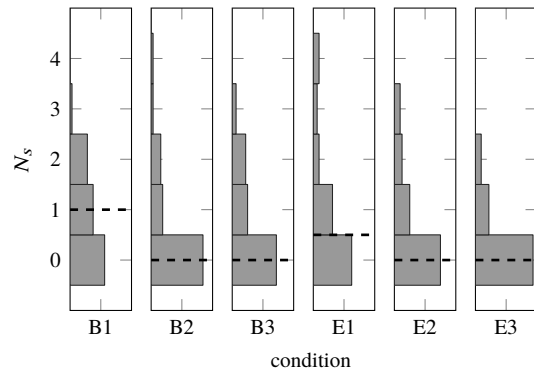
(b) Altitude loss in stall recovery.



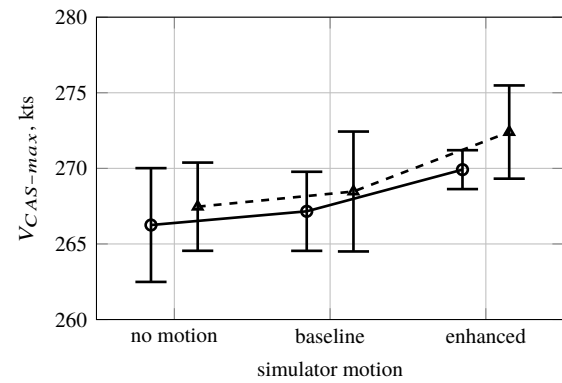
(c) Minimum load factor in stall recovery.



(d) Maximum load factor in stall recovery.



(e) Secondary stick shakers in stall recovery.



(f) Maximum airspeed in stall recovery.

**Fig. 7 Effects of motion setting and aircraft dynamics on objective measures.**

No statistically significant effects were introduced in the altitude loss during the stall recovery,  $\Delta h$ . However, the effect of aircraft dynamics approached statistical significance, with a higher altitude loss in the conditions with enhanced aircraft dynamics (Fig. 7b). The variation in altitude loss is also higher for the enhanced aircraft dynamics compared to the baseline aircraft dynamics, especially with simulator motion.

No significant interaction between aircraft dynamics and motion configuration was introduced in the minimum load factor in the recovery,  $n_{min}$ . The minimum load factor was not statistically significantly affected by the aircraft dynamics; however, it was statistically significantly affected by the motion configuration (Fig. 7c). The minimum load factor increased going from no motion to enhanced motion. Post-hoc analysis with Bonferroni adjustment did not reveal significant differences between any of the condition pairs. The maximum load factor in the recovery,  $n_{max}$ , was not statistically significantly affected by the independent variables (Fig. 7d). Note that the load factor always remained within the critical values ( $-1.0 < n < 2.5$ ).

The number of secondary stick shakers in the recovery,  $N_s$ , was not statistically significantly affected by the aircraft dynamics, but was statistically significantly affected by the motion configuration (Table 4 and Fig. 7e). A post-hoc Wilcoxon test with Bonferroni adjustment revealed that the significant difference was between the no-motion and the enhanced-motion conditions only ( $p = 0.039$ ), with a significant lower number of secondary stick shakers in the enhanced motion configuration. The main effect of experimental condition (CND) was also significant. The post-hoc test revealed no significant differences between any of the condition pairs.

Finally, there was no statistically significant two-way interaction between aircraft dynamics and motion configuration for the maximum calibrated airspeed in the recovery,  $V_{CAS-max}$  (Table 3). The main effect of aircraft dynamics was also not statistically significant. The main effect of motion configuration showed that there was a statistically significant difference in  $V_{CAS-max}$  between motion configurations. The maximum airspeed increased going from no motion to enhanced motion. The post-hoc analysis did not reveal significant differences between any of the condition pairs.

## VII. Discussion

An enhanced motion cueing strategy for stall recovery training in hexapod simulators was developed and evaluated in previous studies in the VMS at NASA Ames Research Center [9–11]. These previous studies showed that pilot control behavior and performance under the enhanced motion was more similar to that under real aircraft motion compared to the baseline motion currently provided by most commercial transport simulators. However, these studies used general aviation pilots in more structured tracking tasks. The current study evaluated the effects of the enhanced motion cueing strategy on pilot stall recovery performance in a level-D full flight simulator. In addition, the effects of enhanced aircraft lateral-directional stall dynamics on stall recovery performance, and the interactions with simulator motion were investigated. Eight commercial airline pilots flew a high-altitude stall recovery task under three different motion configurations (no motion, baseline motion, and enhanced motion) and with two aircraft dynamic models (baseline and enhanced).

The main effects of aircraft dynamics and motion configuration showed that there were statistically significant differences in pilot opinion and performance between different levels. No interactions between aircraft dynamics and motion configuration were found. Motion configuration significantly affected pilots' opinions on the helpfulness of motion in performing the stall-recovery task. Pilots reported that the motion was more helpful in performing the task in the baseline motion condition compared to the no-motion condition. A data trend supporting this result was also identified in the motion ratings, although not by a statistically significant effect. Motion in the enhanced motion condition was reported to be slightly less helpful compared to the baseline motion condition, despite the more accurate motion cues. This was most likely caused by the more abrupt changes in simulator accelerations in this condition due to atmospheric turbulence, a result also found in previous experiments with a similar task [14].

In terms of pilot performance, the maximum roll angle in the stall maneuver and the number of secondary stick shakers in the stall recovery were significantly lower with enhanced motion compared to no motion. Performance under baseline motion was more similar to no motion. These results were also found in previous experiments [14]. This clearly indicates that the enhanced motion allowed pilots to damp the flight path response in a stall recovery, as well as stabilize the progressively less-stable roll dynamics and roll off near stall, more effectively. The minimum load factor and the maximum calibrated airspeed were both significantly higher with better motion fidelity.

The aircraft dynamics significantly affected pilots' opinions on the noticeability of the banking roll off near the stall. Pilots reported that the roll off was more noticeable with the enhanced aircraft dynamics. This is an expected result, as the baseline aircraft dynamics didn't have a roll off. In addition, the maximum roll angle in the stall maneuver was significantly higher with the enhanced aircraft dynamics.

After the experimental matrix was completed, each pilot first flew one more run with the baseline aircraft dynamics and the baseline motion (that is, the configuration representing most heritage simulators), and then one more run with the enhanced dynamics and enhanced motion. This time, they were told the specifics of the condition before the start of the run and were asked to comment on the overall realism after the run was completed. Pilot comments varied, but most pilots commented that aircraft behavior and simulator motion in the baseline condition was as expected in current simulators, that it was pretty realistic, and that they would expect more roll when compared to the real aircraft. Pilots commented that the enhanced condition had more realistic stall behavior, more sideforces than expected, more noticeable turbulence, more realistic motion, and required more roll inputs. One pilot clearly preferred the baseline condition over the enhanced condition.

Despite the limited number of pilots participating in the experiment and the large variability between pilots, significant effects of motion configuration and aircraft dynamics were found between conditions. Additional effects approached statistical significance. These effects would most likely be significant if the statistical power were increased through additional participants. It should also be noted that the simulator used for the experiment has a motion system with 54-inch legs as opposed to the industry standard of 60 inch. In addition, the aircraft model used did not have a clear stall break and responds relatively sluggish compared to smaller aircraft. The benefits of the enhanced motion could potentially be more profound in simulators of smaller aircraft with 60-inch-legged motion systems.

By eliminating the translational accelerations of the center of gravity in the enhanced motion configuration, the fidelity of the remaining motion components at the pilot stations could be increased. However, this also eliminates the sustained g-loads that pilots experience in real stall maneuvers. Because of the limited motion capabilities of hexapod motion platforms (that is, they can generate linear accelerations only for a very brief period), this absence of sustained g-loads was not more pronounced compared to the baseline motion configuration. Presenting pilots with representative g-loads during stall recovery is of great value for stall recovery training [21, 22]. However, this requires centrifuge type simulators or real aircraft, as hexapod simulators are inherently not suitable to produce these sustained accelerations. Furthermore, by eliminating the translational accelerations of the center of gravity, also the sense of deceleration in the approach to the stall could be lost. However, this is highly dependent on the type of stall and pilot performance, and was not noticeable in this experiment.

A no-motion condition was included in the experiment as a baseline to ensure that some perspective was kept on potentially small differences between the two motion configurations. This no-motion condition also did not have any motion effects such as buffeting. Even though this most likely did not affect the results of the experiment, it might have been more appropriate to simulate these cues in the no-motion condition as well, as they are special motion effects generated separately from the main aircraft motions.

The results of this study indicate that the relative minor enhancements to the motion logic of heritage commercial transport simulators presented here can significantly improve pilot performance in high-altitude stall recoveries performed in simulators. This does not necessarily equate to improved stall recovery training. However, previous transfer-of-training experiments in the VMS using the same enhanced motion cueing strategy did indicate improved training and transfer of training compared to motion provided in current commercial transport simulators. Improvements in pilot performance with the enhanced motion configuration might also be found in other flying tasks where the control of aircraft attitude is important. However, as in many other tasks the translational accelerations of the aircraft center of gravity provide useful information to pilots, such as flaring and landing an aircraft, the proposed motion cueing strategy is not a solution for general simulator operations.

## **VIII. Conclusions**

This study used the B747 level-D-certified full flight simulator at NASA Ames Research Center with generic modifications to the aerodynamic model in roll of a very large, generic, four-engine transport aircraft to verify an enhanced motion cueing strategy for stall recovery training. Eight airline transport pilots flew a high-altitude stall recovery task under three different motion configurations: no motion, baseline motion, and enhanced motion. In addition, pilots performed the task with the baseline aircraft dynamics and enhanced aircraft dynamics. Pilot opinion and performance during the stall maneuver were significantly affected by the aircraft dynamics and motion configuration. The maximum roll angle in the stall maneuver was significantly higher with the enhanced aircraft dynamics. Pilots also thought the banking roll off was more noticeable with the enhanced aircraft dynamics. The maximum roll angle in the stall maneuver and the number of secondary stick shakers in the stall recovery were significantly lower with enhanced motion compared to no motion. Performance under baseline motion was more similar to no motion. This clearly indicates that the enhanced motion allowed pilots to damp the flight path response in a stall recovery, as well as

stabilize the progressively less-stable roll dynamics and roll off near stall, more effectively. The minimum load factor and the maximum calibrated airspeed were both significantly higher with better motion fidelity. These results indicate that the relatively minor enhancements to the motion logic of heritage commercial transport simulators presented here can significantly improve pilot performance in simulated stall recoveries, and potentially improve stall recovery training.

### Acknowledgments

This study was supported by Technologies for Airplane State Awareness (TASA), a subproject under NASA's Airspace Operations and Safety Program. The authors would like to thank the simulation engineers and support personnel who contributed to the experiment. We especially thank Richard Blanton from SimLabs at NASA Ames Research Center for his valuable contributions in supporting the experiment. We also thank John Hazelrig for being a test pilot. Finally, we would like to thank the eight pilots who participated in the experiment.

### References

- [1] *Flight Simulation Training Device Qualification Standards for Extended Envelope and Adverse Weather Event Training Tasks, 14 CFR PART 60*, US Department of Transportation, Federal Aviation Administration, 2016.
- [2] Advani, S. K., Schroeder, J. A., and Burks, B., "Global Implementation of Upset Prevention & Recovery Training," *AIAA Modeling and Simulation Technologies Conference*, American Institute of Aeronautics and Astronautics, 2016. doi:10.2514/6.2016-1430.
- [3] Liu, F., and Grant, P., "Ground Based Simulation of Airplane Upset Recovery Using an Enhanced Aircraft Model," *AIAA Modeling and Simulation Technologies Conference*, American Institute of Aeronautics and Astronautics, 2010. doi:10.2514/6.2010-7797.
- [4] Schroeder, J. A., "Research and Technology in Support of Upset Prevention and Recovery Training," *Proceedings of the AIAA Modeling and Simulation Technologies Conference, Minneapolis (MN)*, 2012. doi:10.2514/6.2012-4567.
- [5] Schroeder, J. A., Bürki-Cohen, J., Shikany, D. A., Gingras, D. R., and Desrochers, P., "An Evaluation of Several Stall Models for Commercial Transport Training," *Proceedings of the AIAA Modeling and Simulation Technologies Conference, National Harbor (MD)*, 2014. doi:10.2514/6.2014-1002.
- [6] Grant, P. R., Moszczynski, G. J., and Schroeder, J. A., "Post-stall Flight Model Fidelity Effects on Full Stall Recovery Training," *2018 Modeling and Simulation Technologies Conference*, American Institute of Aeronautics and Astronautics, 2018. doi:10.2514/6.2018-2937.
- [7] Zaal, P. M. T., and Sweet, B. T., "The Challenges of Measuring Transfer of Stall Recovery Training," *Proceedings of the 2014 IEEE International Conference on Systems, Man, and Cybernetics, San Diego, CA*, 2014, pp. 3138–3143. doi:10.1109/SMC.2014.6974410.
- [8] Zaal, P. M. T., Popovici, A., and Zavala, M. A., "Effects of False Tilt Cues on the Training of Manual Roll Control Skills," *Proceedings of the AIAA Modeling and Simulation Technologies Conference, Kissimmee, Florida FL*, 2015. doi:10.2514/6.2015-0655.
- [9] Zaal, P. M. T., and Zavala, M. A., "Effects of Different Heave Motion Components on Pilot Pitch Control Behavior," *AIAA Modeling and Simulation Technologies Conference*, American Institute of Aeronautics and Astronautics (AIAA), 2016. doi:10.2514/6.2016-3371.
- [10] Zaal, P., and Mobertz, X., "Effects of Motion Cues on the Training of Multi-Axis Manual Control Skills," *AIAA Modeling and Simulation Technologies Conference*, American Institute of Aeronautics and Astronautics, 2017. doi:10.2514/6.2017-3473.
- [11] Popovici, A., Zaal, P., and Pieters, M. A., "Time-Varying Manual Control Identification in a Stall Recovery Task under Different Simulator Motion Conditions," *2018 Modeling and Simulation Technologies Conference*, American Institute of Aeronautics and Astronautics, 2018. doi:10.2514/6.2018-2936.
- [12] Zaichik, L. E., Yashin, Y. P., Desyatnik, P. A., and Smaili, H., "Some Aspects of Upset Recovering Simulation On Hexapod Simulators," *Proceedings of the AIAA Modeling and Simulation Technologies Conference, Minneapolis (MN)*, 2012. doi:10.2514/6.2012-4949.
- [13] Ko, S. F., and Grant, P. R., "Development and Testing of an Adaptive Motion Drive Algorithm for Upset Recovery Training," *Proceedings of the AIAA Modeling and Simulation Technologies Conference, Minneapolis (MN)*, 2012. doi:10.2514/6.2012-4947.

- [14] Zaal, P. M. T., Schroeder, J. A., and Chung, W. W., "Objective Motion Cueing Criteria Investigation Based on Three Flight Tasks," *The Aeronautical Journal*, Vol. 121, No. 1236, 2017, pp. 163–190. doi:10.1017/aer.2016.119.
- [15] *Stall Prevention and Recovery Training, AC 120-109A*, US Department of Transportation, Federal Aviation Administration, 2015.
- [16] Cunningham, K., Shah, G. H., Hill, M. A., Pickering, B. P., Litt, J. S., and Norin, S., "A Generic T-Tail Transport Airplane Simulation for High-Angle-of-Attack Dynamics Modeling Investigations," *2018 AIAA Modeling and Simulation Technologies Conference*, American Institute of Aeronautics and Astronautics, 2018. doi:10.2514/6.2018-1168.
- [17] *GTM\_Polysim-Nonlinear GTM Aircraft Polynomial Simulation in MATLAB, Version 2.0*, National Aeronautics and Space Administration, 2018. URL <https://software.nasa.gov/software/LAR-17595-1>, IAR-17595-1.
- [18] Sullivan, B., and Soukup, P., "The NASA 747-400 flight simulator - A national resource for aviation safety research," *Flight Simulation Technologies Conference*, American Institute of Aeronautics and Astronautics, 1996. doi:10.2514/6.1996-3517.
- [19] Zaal, P. M. T., Pool, D. M., de Bruin, J., Mulder, M., and van Paassen, M. M., "Use of Pitch and Heave Motion Cues in a Pitch Control Task," *Journal of Guidance, Control, and Dynamics*, Vol. 32, No. 2, 2009, pp. 366–377. doi:10.2514/1.39953.
- [20] Field, A., *Discovering Statistics Using SPSS*, 2<sup>nd</sup> ed., ISM Introducing Statistical Methods, SAGE Publications Ltd., 1 Oliver's Yard, 55 City Road, London EC1Y 1SP, 2005.
- [21] Comtois, P. W., and Glaser, S. T., "Effectiveness of Sustained G Simulation in Loss of Control and Upset Recovery Training," *Proceedings of the AIAA Modeling and Simulation Technologies Conference, Toronto, Ontario, Canada*, 2010. doi:10.2514/6.2010-7798.
- [22] Nooij, S. A. E., Wentink, M., Smaili, H., Zaichik, L., and Groen, E. L., "Motion Simulation of Transport Aircraft in Extended Envelopes: Test Pilot Assessment," *Journal of Guidance, Control, and Dynamics*, 2016, pp. 1–13. doi:10.2514/1.g001790.